Spatial involute gearing - a new type of skew gears

Hellmuth Stachel
Institute of Discrete Mathematics and Geometry
Vienna University of Technology
Wiedner Hauptstr. 8-10/104, A 1040 Wien, AUSTRIA
stachel@dmg.tuwien.ac.at

Abstract

This is a geometric approach to spatial involute gearing which has recently been developed by Jack Phillips [4]. Due to Phillips' fundamental theorems helical involute gears for parallel axes (Fig. 2) serve also as tooth flanks for a uniform transmission between skew axes, and the transmission ratio is even independent of the relative position of the axes.

1. Introduction

The function of a gear set is usually to transmit a rotary motion of the input wheel Σ_1 about the axis p_{10} with angular velocity ω_{10} to the output wheel Σ_2 rotating about p_{20} with ω_{20} in a uniform way, i.e., with a constant transmission ratio

$$i := \omega_{20} / \omega_{10} = \text{const}. \qquad (1)$$

According to the relative position of the gear axes p_{10} and p_{20} we distinguish the following types;

a) Planar gearing (spur gears) for parallel axes p_{10}, p_{20},

b) spherical gearing (bevel gears) for intersecting axes p_{10}, p_{20}, and

c) spatial gearing for skew axes p_{10}, p_{20}, in particular worm gears for orthogonal p_{10}, p_{20}.

1.1 Planar gearing: In the case of parallel axes p_{10}, p_{20} we confine us to a perpendicular plane where two systems Σ_1, Σ_2 are rotating against the gear box Σ_0 about centers 10, 20 with velocities ω_{10}, ω_{20}, respectively. Two curves $c_1 \subset \Sigma_1$ and $c_2 \subset \Sigma_2$ are conjugate profiles when they are in permanent contact during the transmission, i.e., (c_2, c_1) is a pair of enveloping curves under the relative motion Σ_2 / Σ_1. Due to a standard theorem from plane kinematics (see, e.g., [2,8]) the common normal at the point E of contact must pass through the pole 12 of this relative motion (Fig. 1). Due to the planar Three-Pole-Theorem this point 12 divides the segment 01 02 at the constant ratio i and is therefore fixed in Σ_0. We summarize:

Theorem 1 (Fundamental law of planar gearing): *The profiles $c_1 \subset \Sigma_1$ and $c_2 \subset \Sigma_2$ are conjugate if and only if the common normal e (= meshing normal) at the point E of contact (= meshing point) passes through the relative pole* 12.

Due to L. Euler (1765) planar involute gearing (see Fig. 1, cf. [2,8]) is characterized by the property that with

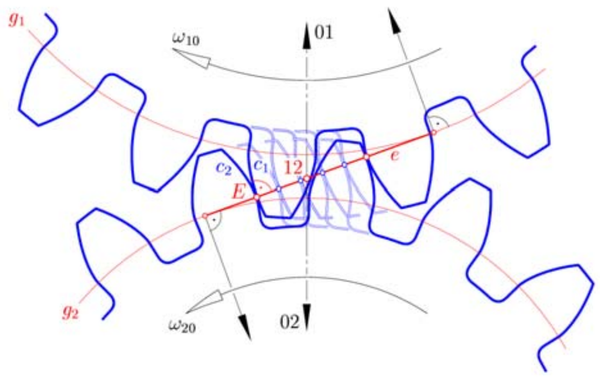

Fig. 1 Planar involute gearing

respect to Σ_0 all meshing normals e are coincident. This implies

(i) The profiles are involutes of the base circles.

(ii) For constant driving velocity ω_{10} the meshing point E traverses e relative to Σ_0 with constant velocity.

(iii) The transmitting force has a fixed line e of action.

(iv) The transmission ratio i depends only on the dimension of the curves c_2, c_1 and not on their relative position. Therefore this planar gearing remains independent of errors upon assembly.

It will turn out that all these properties are still valid for spatial involute gears. Helical gears over involute spur gears (Fig. 2) have helical torses (developables) (see Fig. 3) as tooth flanks.

Fig. 2: Helical gears

1.2 Basics of spatial gearing: In the sequel we present a geometric way to spatial gearing. Readers who prefer the analytic approach are referred to [6] where the same topic is treated using dual vectors [7,3,5].

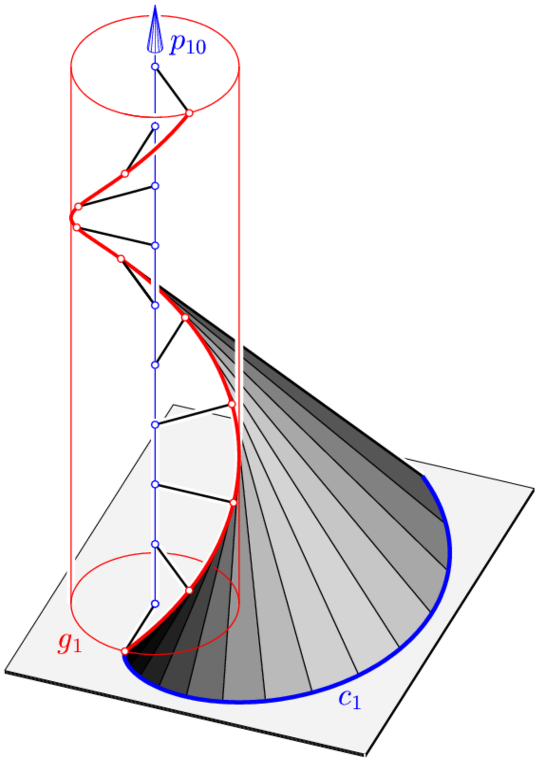

Fig. 3: Helical involute (torse) swept by tangent lines of a helix; the cross section c_1 is a planar involute

We start with an important

Lemma 1: *Let the tooth flanks $\Phi_1 \subset \Sigma_1$ and $\Phi_2 \subset \Sigma_2$ transmit the rotation of wheel Σ_1 about p_{10} to the rotation of wheel Σ_2 about p_{20}. Then one single point E of contact between Φ_1 and Φ_2 defines the instantaneous transmission ratio $i = \omega_{20}/\omega_{10}$ uniquely. i depends only on the meshing normal e by*

$$i = \frac{\omega_{20}}{\omega_{10}} = \frac{\hat{\alpha}_1 \sin\alpha_1}{\hat{\alpha}_2 \sin\alpha_2}. \qquad (2)$$

Here α_j and $\hat{\alpha}_j$ (see Fig. 6) denote the signed distance and the angle between e and each axis p_{j0}.

Proof: Let ${}_E\mathbf{v}_0$ denote the instantaneous velocity vector of E against Σ_0 (Fig. 4). Then this vector is the sum of the guiding velocity ${}_E\mathbf{v}_{j0}$ of E under the rotation Σ_j/Σ_0 and the relative velocity ${}_E\mathbf{v}_j$ of E with respect to the tooth flank Φ_j. This gives

$${}_E\mathbf{v}_0 = {}_E\mathbf{v}_{10} + {}_E\mathbf{v}_1 = {}_E\mathbf{v}_{20} + {}_E\mathbf{v}_2\,. \qquad (3)$$

Since ${}_E\mathbf{v}_1$ and ${}_E\mathbf{v}_2$ are parallel to the common tangent plane ε, the components of ${}_E\mathbf{v}_1$ and ${}_E\mathbf{v}_2$ in direction of the meshing normal e must be equal.

In order to obtain these components, we inspect the first wheel and choose e and p_{10} parallel to the image plane of the front view (Fig. 4). If φ denotes the angle between ${}_E\mathbf{v}_{10}$ and the front plane, then the front view ${}_E\mathbf{v}_{10}''$ has the length

$$r\,\omega_{10}\cos\varphi = (r\cos\varphi)\,\omega_{10} = \hat{\alpha}_1\,\omega_{10}$$

with the distance $r = \overline{E\,p_{10}}$. We note that the length of ${}_E\mathbf{v}_{10}''$ is the same for all points of e. Its component in the specified direction of e reads $-\omega_{10}\,\hat{\alpha}_1 \sin\alpha_1$. This yields

$$-\omega_{10}\,\hat{\alpha}_1 \sin\alpha_1 = -\omega_{20}\,\hat{\alpha}_2 \sin\alpha_2 \qquad (4)$$

which is equivalent to (2).

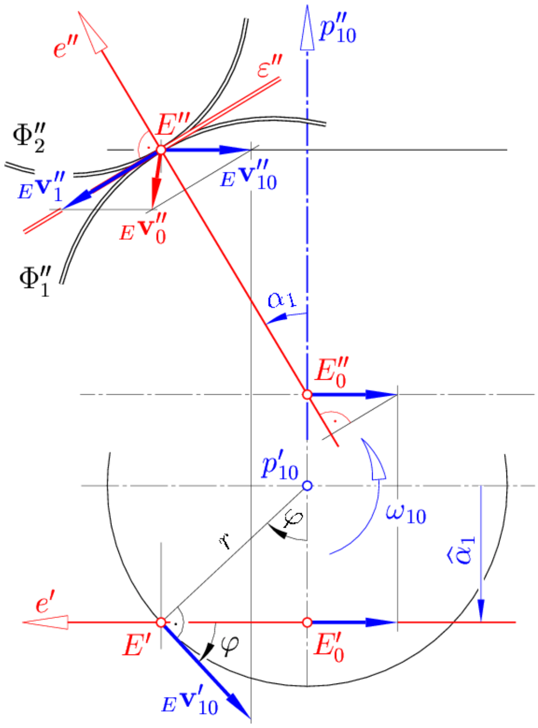

Fig. 4: Proof of Lemma 1

It should be noted that for any two directed lines g and h (Fig. 5) a signed distance $\hat{\varphi}$ and angle φ according to the right-hand-rule is defined, provided the common normal n is directed, too. When the orientation of n is reversed then φ and $\hat{\varphi}$ change their sign. When the orientation either of g or of h is reversed then φ has to be replaced by $\varphi + \pi \pmod{2\pi}$.

In analogy to the planar case we obtain from Lemma 1

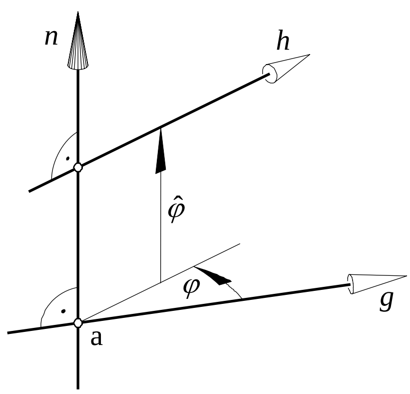

Fig. 5: Distance $\hat{\varphi}$ and angle $\underline{\varphi}$ between g and h

Theorem 2 (Fundamental law of spatial gearing): *The tooth flanks $\Phi_1 \in \Sigma_1$ and $\Phi_2 \in \Sigma_2$ are conjugate if and only if at each meshing point E the meshing normal e obeys eq.* (2).

Remark: Eq. (2) as well as (4) characterizes the linear line complex of instantaneous path normals of the relative motion Σ_2/Σ_1. The spatial Three-Pole-Theorem states (cf. [1,5]): *If for three given systems Σ_0, Σ_1, Σ_2 the dual vectors $\underline{\mathbf{q}}_{10}$, $\underline{\mathbf{q}}_{20}$ are the instantaneous screws of Σ_1/Σ_0, Σ_2/Σ_0, resp., then*

$$\underline{\mathbf{q}}_{21} = \underline{\mathbf{q}}_{20} - \underline{\mathbf{q}}_{10}$$

is the instantaneous screw of the relative motion Σ_2/Σ_1.

As a consequence, if a line n which intersects the ISAs p_{10} of Σ_1/Σ_0 and p_{20} of Σ_2/Σ_0 orthogonally, then it does the same with the axis p_{21} of Σ_2/Σ_1, provided $\omega_{21} \neq 0$ (note the three axes in Fig. 11).

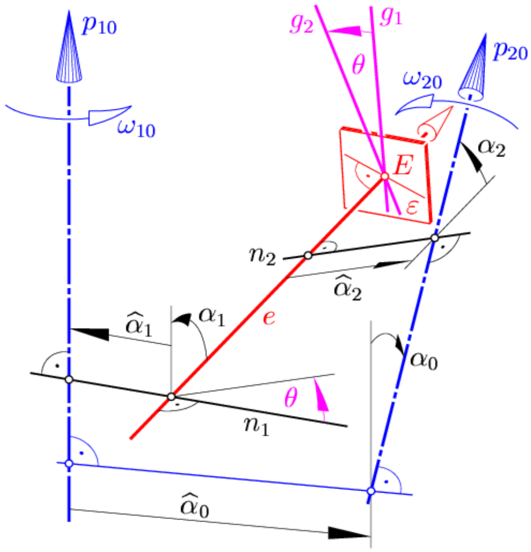

Fig. 6: Relative position of the meshing normal e

2. Spatial involute gearing

Spatial involute gearing is characterized in analogy to the planar case as follows (cf. Phillips [6]): All meshing normals e are coincident in Σ_0 – and skew to p_{10} and p_{20}. We exclude also perpendicularity between e and one of the axes.

According to (2) a constant contact normal e implies already a constant transmission ratio i.

2.1 Slip tracks: First we focus on the paths of the meshing point E relative to the wheels Σ_1, Σ_2. These paths are called slip tracks s_1, s_2.

Σ_1/Σ_0 is a rotation about p_{10}, and with respect to Σ_0 point E is placed on the fixed line e. Therefore – conversely – the slip track s_1 is located on the one-sheet hyperboloid Π_1 of revolution through e with axis p_{10}.

On the other hand, the slip track s_1 is located on the tooth flank Φ_1, and for each posture of Φ_1 line $e \subset \Sigma_0$ is orthogonal to the tangent plane ε at the instantaneous point E of contact (see Fig. 6).

Therefore the line tangent to the slip track s_1 is orthogonal to e. This gives the result:

Lemma 2: *The path s_1 of E relative to Σ_1 is an orthogonal trajectory of the e-regulus on the one-sheet hyperboloid Π_1 through e with axis p_{10}.*

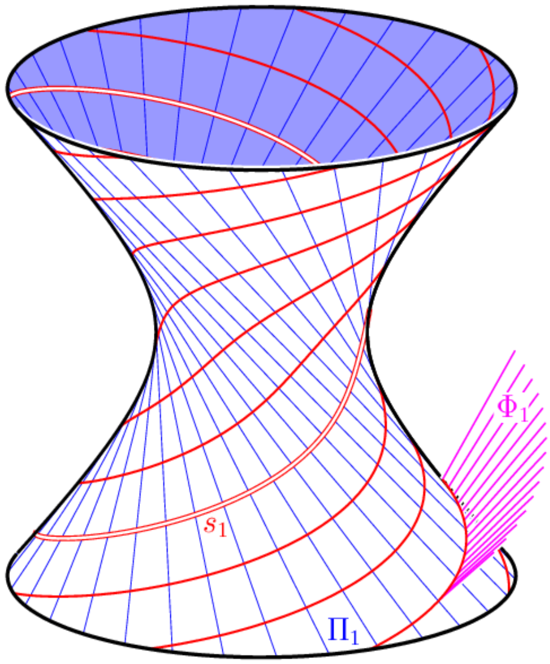

Fig. 7: The slip track s_1 as an orthogonal trajectory of one regulus on the one-sheet hyperboloid Π_1

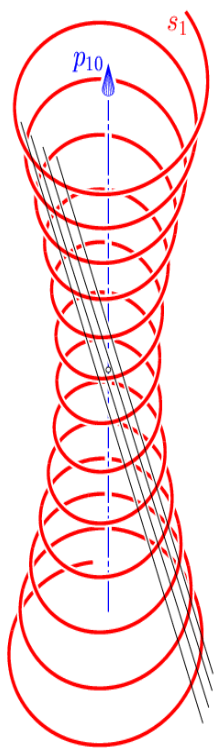

Fig. 8: Slip track s_1 as „bed-spring curve“

A parameter representation of s_1 can be found in [6].

2.2 The tooth flanks: Phillips' spatial involute gearing offers only single point contact between the teeth. So, only the portion of the tooth flank close to the slip track is of relevance. The simplest tooth flank is the envelope Φ_1 of the plane ε of contact in Σ_1, while the meshing point E is traversing the slip track s_1. We prove in the sequel that this is a helical torse (see Fig. 10):

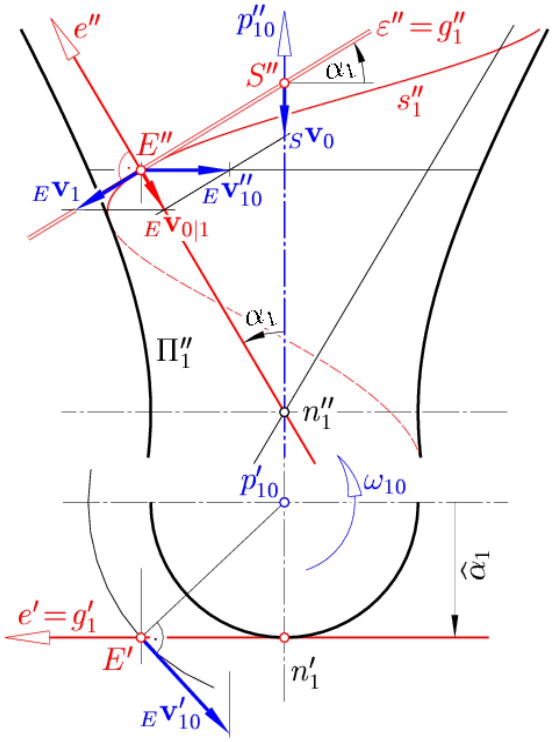

Fig. 9: Proving that the envelope of ε along the slip track s_1 is a helical torse Φ_1 (Lemma 3)

Let the wheel Σ_1 with Φ_1 rotate with constant angular velocity ω_{10}, while simultaneously the meshing point E traverses s_1 in such a way that with respect to to Σ_0 point E remains on e. Then E moves along e with the constant velocity

$$_E v_{0|1} = -\omega_{10}\,\hat{\alpha}_1 \sin\alpha_1 = \text{const}. \tag{5}$$

relatively to Σ_0 (see Fig. 9). This implies that also the tangent plane ε moves with this constant velocity along e. Hence, ist point S of intersection with the axis p_{10} has a constant velocity, too, namely

$$_S v_0 = -\omega_{10}\,\hat{\alpha}_1 \tan\alpha_1 \tag{6}$$

How is the movement of ε relative to Σ_1? The plane rotates about p_{10} with angular velocity $-\omega_{10}$ and translates at the same time with velocity ${}_S\mathbf{v}_0$ along p_{10}. The envelope is a helical torse Φ_1. Its cuspical edge, a helix (see Fig. 3), has the radius $r_1 := \hat{\alpha}_1$ and the pitch

$$h_1 = \frac{_S v_0}{-\omega_{10}} = \hat{\alpha}_1 \tan\alpha_1 . \tag{7}$$

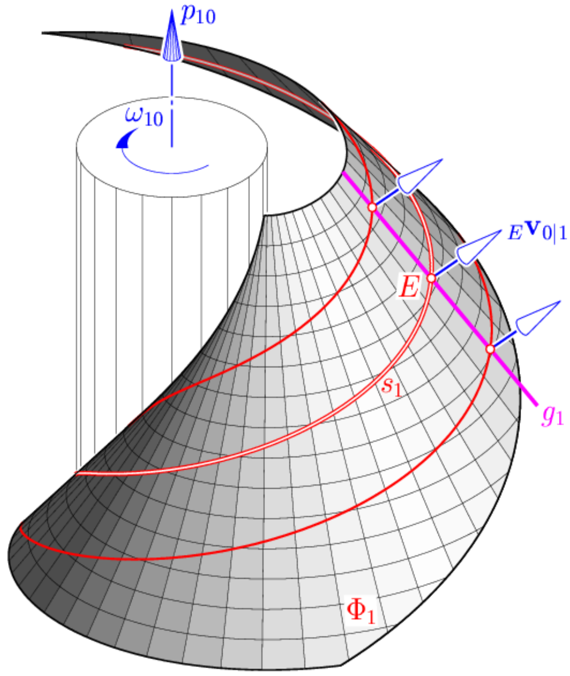

Fig. 10: Helical torse Φ_1 with slip track s_1 and generator g_1

This proves that Φ_1 is uniquely defined by one single meshing normal e – up to rotations about p_{10}. Thus we got

Lemma 3: *The slip track s_1 is located on a helical torse Φ_1 with the pitch $\hat{\alpha}_1 \tan\alpha_1$. At each meshing point $E \in s_1$ there is an orthogonal intersection between Φ_1 and the one-sheet hyperboloid Π_1 of Lemma 2 (note Fig. 7).*

2.3 Fundamental theorems: We summarize:

Theorem 3 (Phillips' 1st Fundamental Theorem): *The helical torses Φ_1, Φ_2 are conjugate tooth flanks for a spatial gearing with single point contact such that all meshing normals coincide with a line e fixed in Σ_0.*

The following theorem completes the confirmation that the advantages (ii) – (iv) of planar involute gearing as listed above are still valid for spatial involute gearing:

Theorem 4 (Phillips' 2nd Fundamental Theorem): *If two given helical torses Φ_1, Φ_2 are placed in mutual contact at point E and if their axes are kept fixed in this position, then Φ_1 and Φ_2 serve as tooth flanks for a uniform transmission whether the axes are parallel, intersecting or skew. According to (2) the transmission ratio i depends only on the dimensions r_1, h_1, r_2, h_2 of Φ_1 and Φ_2 and not on their relative position. Therefore this spatial gearing remains independent of errors upon assembly.*

Proof: We start in a pose where the two flanks Φ_1, Φ_2 are in contact at point E. If then the two flanks Φ_1, Φ_2 rotate with constant angular velocities ω_{10}, ω_{20} about their axes p_{10}, p_{20} and point E traverses relatively the slip tracks s_1, s_2 with appropriate velocities (see Fig. 9), then with respect to Σ_0 point E traces e with the velocities

$$_E v_{0|1} = -\omega_{10}\hat{\alpha}_1 \sin\alpha_1 \quad \text{and} \quad _E v_{0|2} = -\omega_{20}\hat{\alpha}_2 \sin\alpha_2 ,$$

due to (5). By (2) or (4) these velocities are equal at any moment if and only if the transmission ratio i remains constant. Hence the initial contact between Φ_1 and Φ_2 at E is preserved under the simultaneous rotations of both wheels with the ratio (2).

Theorem 5 ([6]): *During the uniform transmission by two given helical involutes Φ_1, Φ_2 the angle θ between the generators $g_1 \subset \Phi_1$ and $g_2 \subset \Phi_2$ at the meshing point E remains constant (Fig. 13). This angle is congruent to the angle made by the normal lines n_1, n_2 between the meshing normal e and the axes p_{10}, p_{20}, respecitively (see Fig. 6).*

Proof: Both generators g_1, g_2 as well the common normals n_1, n_2 are perpendicular to the meshing normal e, which is fixed in Σ_0 (Fig. 6). In addition, g_1 is orthogonal to n_1 (Fig. 9) and g_2 orthogonal to n_2. So we get congruent angles $\theta = \angle g_1 g_2 = \angle n_1 n_2$.

In the special case $\theta = 0$ we obtain: If according to Theorem 4 the two helical torses are placed such that they are in contact along a straight line g, then this line contact is preserved during the transmission.

7. Conclusion

It is proved in a geometric way that helical torses (developables) surprisingly serve as tooth flanks not only for spur gears but also for skew gears. And in the skew case they have still the important property that the transmission ratio is not sensitive against errors of assembly.

References

[1] Husty, M., Karger, A., Sachs, H., and Steinhilper, W., Kinematik und Robotik, Springer-Verlag, Berlin Heidelberg (1997).

[2] Litvin, F. L., Gear Geometry and Applied Theory, Prentice Hall, Englewood Cliffs, N.J. (1994).

[3] McCarthy, J. M., Geometric Design of Linkages, Springer-Verlag, New York (2000).

[4] Phillips, J., General Spatial Involute Gearing, Springer Verlag, New York (2003).

[5] Stachel, H., "Instantaneous spatial kinematics and the invariants of the axodes", Proceedings Ball 2000 Symposium, Cambridge (2000), no. 23.

[6] Stachel, H., "On Jack Phillips' Spatial Involute Gearing", Proc. 11th ICGG, Guangzhou, China (2004).

[7] Veldkamp, G. R., "On the Use of Dual Numbers, Vectors, and matrices in Instantaneous Spatial Kinematics", Mech. and Mach. Theory 11, 141-156 (1976).

[8] Wunderlich, W., Ebene Kinematik, Bibliographisches Institut, Mannheim (1970).

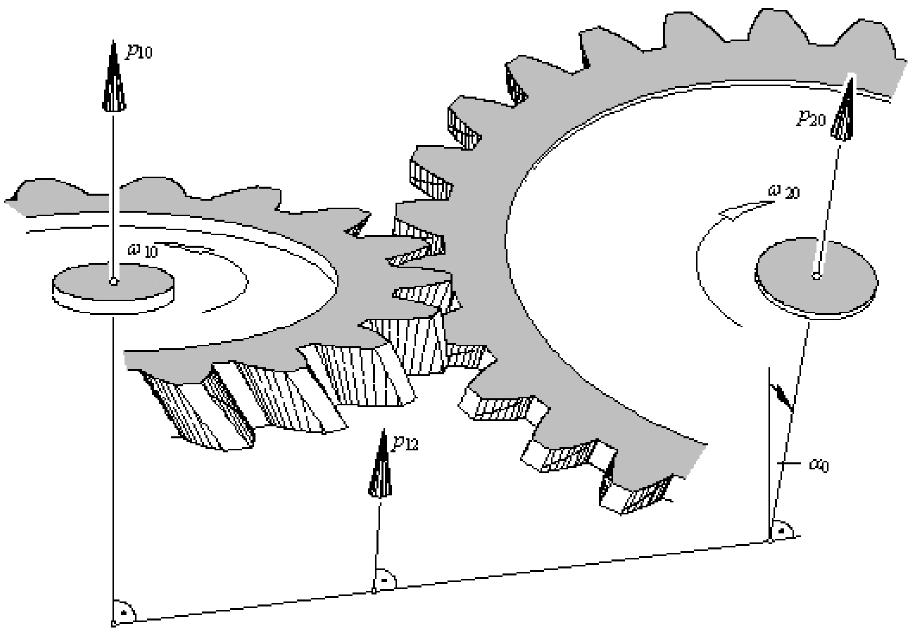

Fig. 11: Spatial involute gearing together with the effective slip tracks on the flanks. List of dimensions: Transmission ratio $i = -2/3$, numbers of teeth: $z_1 = 18$, $z_2 = 27$; contact ratio 1.095; dual angle between p_{10} and p_{20}: $\alpha_0 = 21.35°$, $\hat{\alpha}_0 = 117.01$; dual angles between p_{i0} and the fixed contact normal e: $\alpha_1 = -60.0°$, $\hat{\alpha}_1 = 45.0$, $\alpha_2 = 76.98°$, $\hat{\alpha}_2 = 60.0$, and (compare Fig. 3) angle $\theta = 14.0°$.

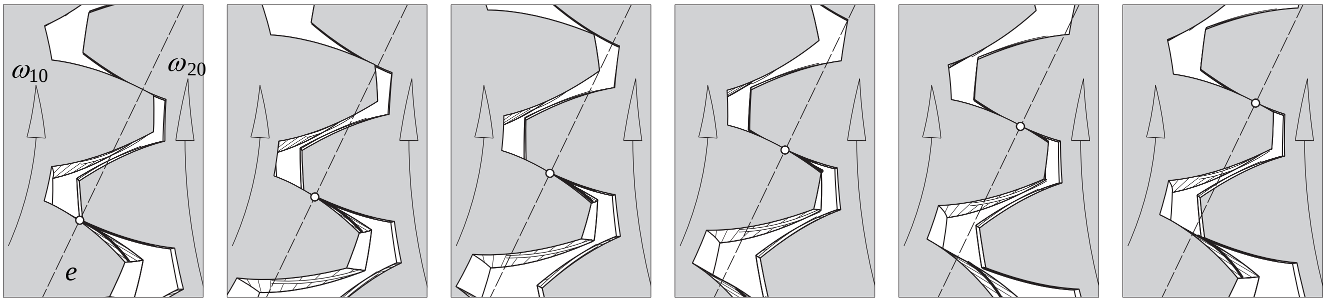

$\varphi_{10} = 0°$ $\varphi_{10} = 3.6°$ $\varphi_{10} = 7.2°$ $\varphi_{10} = 10.8°$ $\varphi_{10} = 14.4°$ $\varphi_{10} = 18.0°$

Fig. 12: Different postures of meshing involute teeth for inspecting the backlash. e is the line of contact. Interval of the input angle $\Delta\varphi_{10} = 3.6°$, interval of the output angle $\Delta\varphi_{20} = -2.4°$.

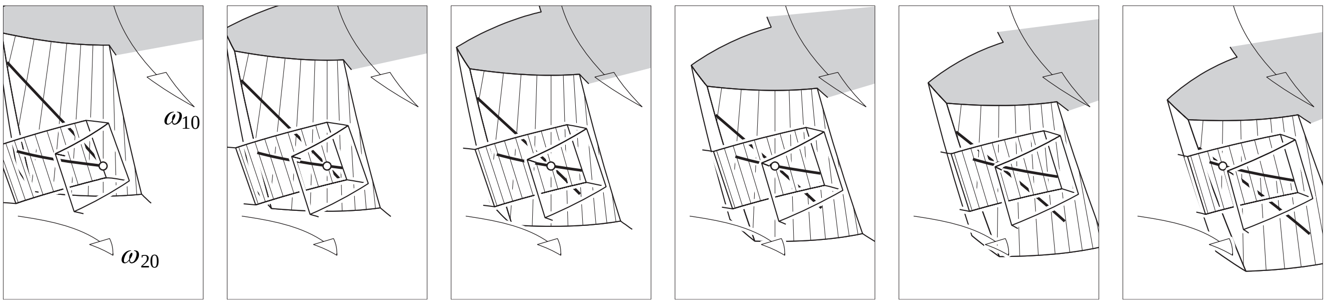

Fig. 13: Different postures of meshing involute gear flanks together with the effective slip tracks, seen in direction of the contact normal e. The second wheel is displayed as a wireframe.